ISSN 0006-2979, Biochemistry (Moscow), 2022, Vol. 87, No. 10, pp. 1138-1148 © Pleiades Publishing, Ltd., 2022.
Russian Text © The Author(s), 2022, published in Biokhimiya, 2022, Vol. 87, No. 10, pp. 1434-1446.

Effect of Dipyridamole on Membrane Energization and Energy Transfer in Chromatophores of *Rba. sphaeroides*

Peter P. Knox[1,a]*, Eugene P. Lukashev[1], Boris N. Korvatovskii[1], Nuranija Kh. Seifullina[1], Sergey N. Goryachev[1], Elvin S. Allakhverdiev[2], and Vladimir Z. Paschenko[1]

[1] *Faculty of Biology, Lomonosov Moscow State University, 119991 Moscow, Russia*
[2] *Russian National Medical Research Center of Cardiology, 121552 Moscow, Russia*
[a] *e-mail: knox@biophys.msu.ru*

Received June 7, 2022
Revised August 24, 2022
Accepted August 24, 2022

Abstract—Effect of dipyridamole (DIP) at concentrations up to 1 mM on fluorescent characteristics of light-harvesting complexes LH2 and LH1, as well as on conditions of photosynthetic electron transport chain in the bacterial chromatophores of *Rba. sphaeroides* was investigated. DIP was found to affect efficiency of energy transfer from the light-harvesting complex LH2 to the LH1–reaction center core complex and to produce the long-wavelength ("red") shift of the absorption band of light-harvesting bacteriochlorophyll molecules in the IR spectral region at 840-900 nm. This shift is associated with the membrane transition to the energized state. It was shown that DIP is able to reduce the photooxidized bacteriochlorophyll of the reaction center, which accelerated electron flow along the electron transport chain, thereby stimulating generation of the transmembrane potential on the chromatophore membrane. The results are important for clarifying possible mechanisms of DIP influence on the activity of membrane-bound functional proteins. In particular, they might be significant for interpreting numerous therapeutic effects of DIP.

DOI: 10.1134/S0006297922100078

Keywords: chromatophores, membrane energization, energy transfer, dipyridamole

INTRODUCTION

Dipyridamole is a modified purine (2,6-bis(diethanolamino)-4,8-dipiperidino-pyrimidino (5,4-d)pyrimidine). Structural formula of the molecule is shown below (scheme).

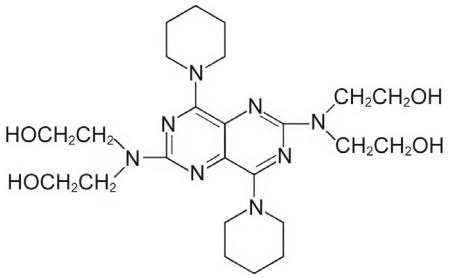

The chemical structural formula of dipyridamole

This drug is widely used in medicine as a coronary vasodilator and antithrombotic agent that inhibits platelet aggregation. The proposed mechanism of its antithrombotic activity is inhibition of the platelet activation that alters the shape of platelets, thus initiating their aggregation. This process results from the action of dipyridamole (DIP) on phosphodiesterase that regulates the signal transduction pathway mediated by cyclic nucleotides (cGMP and cAMP) [1]. DIP also acts as an effective inhibitor of the transmembrane P-gp protein, an ATP-dependent pump of lipophilic compounds that pumps antitumor drugs out of cancer cells [2, 3]. It has been suggested that suppression of this membrane transporter may stem from the direct inhibition of the binding sites of transported substrates or from disorders in

Abbreviations: BChl, bacteriochlorophyll; DIP, dipyridamole; LH1 and LH2, light-harvesting complexes; P, photoactive bacteriochlorophyll; Q_A, primary quinone acceptor; Q_B, secondary quinone acceptor; RC, reaction center; TMPD-H_2, N,N,N',N'-tetramethyl-p-phenylenediamine reduced by ascorbate.

* To whom correspondence should be addressed.

the coupled process of ATP binding and hydrolysis [4]. DIP also promotes a few other biological activities including anti-inflammatory, antioxidant, and antiviral functions. Because of the wide range of pharmacological activity of DIP (vasodilating, antithrombotic, anti-inflammatory, and antioxidant), there are theoretical bases for the use of dipyridamole as a therapeutic agent in the treatment of patients with COVID-19. The coronavirus-19 disease begins as a respiratory infection but it may be accompanied by a hypercoagulable state, severe inflammation due to excessive cytokine production, and by the potentially significant oxidative stress [5, 6]. However, despite the long-term medical use of dipyridamole, the detailed mechanisms of its numerous therapeutic effects remain unclear.

In our previous works we studied the mechanisms of DIP interaction with biological structures by analyzing effects of dipyridamole and its derivatives on photoinduced electron and proton transport in the photosynthetic reaction centers (RC) of the purple bacteria and in the purple membranes of the bacteriorhodopsin-containing halobacteria [7-9]. In these studies, the transmembrane photosensitive protein complexes were used as convenient informative test systems for studying molecular mechanisms of the dipyridamole impact on membrane proteins. It was shown that, in the RC preparations isolated from *Rba. sphaeroides*, DIP accelerates dark recombination between the photooxidized bacteriochlorophyll (BChl) dimer P^+ and the reduced primary quinone acceptor Q_A^-. In the chromatophore membranes of these bacteria, dipyridamole slows down formation of the fully reduced secondary quinone acceptor, Q_BH_2 hydroquinone, that transfers reducing equivalents from the RC protein into the photosynthetic membrane. The effect of DIP on bacteriorhodopsin photocycle was manifested by the decelerated decay of the M-intermediate, which is associated with the re-protonation of the Schiff base.

As noted above, DIP exhibits also antioxidant properties, inhibiting, in particular, lipid peroxidation due to its capability of one- and two-electron oxidation [10-12]. Therapeutic effects of this chemical might be due to its antioxidant capacity [10, 13]. Influence of antioxidant agents on the P-gp protein was shown using several flavonoids as examples [14]. In our previous studies we showed the possibility of generating DIP cation radical during DIP interaction with both isolated RC protein–pigment complexes of *Rba. sphaeroides* and with the chromatophore membranes of these bacteria [15, 16]. We also suggested that the putative electron–donor properties of DIP provide prerequisites for energization of the energy-coupling membranes [16].

The effects of DIP on functional biological membranes and interactions of their integral components clearly deserve further study. The aim of this work was to study effects of DIP on the energy transfer from light-harvesting protein–pigment complexes to photosynthetic RC in the *Rba. sphaeroides* bacteria and to characterize electron-donor properties of DIP using high-resolution fluorescence and absorption spectroscopy among other methods.

MATERIALS AND METHODS

Photosynthetic membranes of chromatophores from the wild-type strain of purple nonsulfur bacteria *Rhodobacter sphaeroides* were isolated using fresh cells of a 5- to 6-day culture after washing the cells with sodium phosphate buffer (100 mM, pH 7.5). Following ultrasonic disintegration of cells, the remaining unbroken bacterial cells and large particles were separated by centrifugation at 40,000*g* for 15 min; chromatophores were obtained by centrifugation of the supernatant at 144,000*g* for 120 min with L5-50 Beckman ultracentrifuge. Chromatophores were suspended in a 20 mM sodium phosphate buffer, pH 7.5. Before measurements, they were diluted with a buffer to ~10 μM concentration of the photoactive pigment. The preparations exhibited well pronounced photoinduced electron transport activity despite the initially low rate of cyclic electron flow. The latter feature was apparently related to a significant loss of cytochrome c_2, a water-soluble mobile electron carrier.

Dipyridamole is poorly soluble in water but its solubility increases in the acidic pH range. Therefore, the 20 mM DIP stock solution was acidified to pH 4.5. However, even the highest final concentration of DIP (1 mM) obtained by addition of 50 μl DIP to 950 μl chromatophores had no significant influence on the pH value in the sample because of the high buffer capacity of the suspension medium.

An aqueous solution of TMPD (N,N,N',N'-tetramethyl-p-phenylenediamine, Sigma-Aldrich, USA) at a concentration from 1 μM to 1 mM in combination with sodium ascorbate (sodium L-ascorbate, Sigma-Aldrich) was used as an exogenous electron donor. Sodium L-ascorbate was added at a concentration one order of magnitude higher than the concentration of TMPD.

Absorption spectra were recorded using a modified Hitachi-557 spectrophotometer (Japan); fluorescence spectra were recorded using a Fluorolog 3 spectrofluorometer (Horiba Jobin Yvon, Japan) equipped with a cooled Hamamatsu-5509 photomultiplier tube highly sensitive in the IR spectral range. Fluorescence was excited at the Soret absorption band (400 nm) of porphyrin pigments. Fluorescence decay kinetics were recorded using photon counting at a wavelength of 880 nm with a Becker & Hickl (Germany) system in the time-correlated single photon counting (TCSPC) mode. An HPM-100-07 hybrid photodetector provided instrumental function of the recording system of approximately 16 ps. A Tema-150 femtosecond laser system (Avesta-Proekt, Russia) that generated light pulses with a wavelength of 400 nm, duration of 300 fs,

and repetition rate of 80 MHz (the average radiation power was 2.8 W was used as an excitation light source; energy of a single laser pulse was 34 nJ). In our experiments, energy of the excitation light pulses was reduced by means of neutral light filters to a level determined by the sensitivity of the recording system; average radiation power density was $3 \cdot 10^{-4}$ W/cm^2. A two-exponential approximation was used to fit fluorescence kinetics.

Photoinduced absorbance changes in the region of 740-920 nm were recorded under stationary monochromatic illumination at 10 nm intervals using a single-beam differential spectrophotometer with mechanical light modulation. The sample was illuminated for 5 s with red light ($\lambda > 620$ nm). Differential "light minus dark" absorbance spectrum was constructed from the data points using the Origin 8.1 program (OriginLab, USA) and the "spline" smoothing function.

Absorbance changes induced by a single flash (532 nm, duration 7 ns, pulse energy 10 mJ, YAG-Nd laser LS-2131M LOTIS TII, The Republic of Belarus) were recorded with a flash photolysis system featuring double monochromatization of the probing light. The signal-to-noise ratio was improved by averaging 50-100 individual signals with a Gage Octopus CompuScope 8327 analog-to-digital converter (Canada). Multiexponential approximation of kinetic curves was carried out with the Origin 8.1 program (OriginLab).

All measurements were repeated at least three times, and the results were averaged. Data represent mean values and their standard errors.

RESULTS

Photosynthetic apparatus of the purple bacterium *Rba. sphaeroides* contains light-harvesting complexes of two types (LH1 and LH2), cytochrome bc_1 reaction center complexes, and ATP synthetase [17]. In the membrane, the RC and LH1 form an LH1–RC complex, in which each RC is surrounded by an LH1 ring protein structure containing 32 linked BChl molecules. The Q_y absorption band of LH1 has a maximum at 875 nm; fluorescence spectrum of this complex shows a peak at 885 nm. In contrast to LH1, the LH2 complex includes two spectrally different types of BChl molecules. The short-wavelength antenna type is formed by nine BChl molecules that absorb light quanta at 800 nm; the remaining 18 BChl molecules form a closely packed structure that absorbs light at 850 nm. Excitation energy is rapidly transferred from the B800 ring complex to the ring of the B850 complex that is able to emit fluorescence. The peak of B850 fluorescence spectrum is at 860 nm [18].

Kinetics of the fluorescence decay in the isolated chromatophores of *Rba. sphaeroides* cells that were grown under standard conditions contains usually three components with lifetimes ~100, 200-300, and 700-1000 ps [19, 20]. The authors believed that the fast component with ~100 ps lifetime is associated with the excitation trapping from LH1. The second component is related either to the energy transfer from LH2 to LH1 or to the charge recombination in the P^+H^- pair, where P is photoactive BChl dimer and H is bacteriopheophytin. The third long-lived component reflects fluorescence lifetime of the LH2 complexes that are not bound to LH1. It should be noted that the energy connectivity of LH2–LH1 complexes determines both lifetime of LH2 fluorescence and probability of occupation of LH1 complexes [21]. The kinetics of fluorescence decay in chromatophores of *Rba. sphaeroides* was analyzed in detail in our work [22].

The absorption spectra of *Rba. sphaeroides* chromatophores showed no apparent differences under the control conditions and in the presence of DIP (0.25, 0.5, and 1 mM). At the same time, characteristics of the chromatophore fluorescence were evidently affected by DIP. In the control samples (Fig. 1), the main maximum at ~890 nm is due to the fluorescence of LH1 complex that accepts energy absorbed by the light-harvesting pigments of the LH2 chromatophore complex. The well-defined shoulder at ~855 nm represents contribution of the LH2 fluorescence to the fluorescence emission spectrum. Figure 1 shows fluorescence spectra of the chromatophores and the results of their decomposition into two Gaussian components with maxima at ~890 nm and ~855 nm corresponding to the emission of LH1 and LH2 complexes, respectively. Comparison of the spectra shows that the fluorescence of LH2 increases after addition of 1 mM DIP. In the control sample, the ratio of areas under the Gaussian curves of LH1 and LH2 fluorescence spectra was approximately 35, but this value decreased to 20 in the presence of DIP. Addition of TMPD-H_2 had no influence on the fluorescence spectra (data not shown). An even more significant increase in the intensity of LH2 fluorescence and, accordingly, relative decrease in the LH1 fluorescence were found in our recent work dealing with the effects of cationic antiseptics on the energy transfer in the same preparations of bacterial chromatophores [22]. These changes were found to arise from disruption of the functional connectivity between the peripheral pigment–protein complexes LH2 and the core complexes LH1–RC manifested by the reduced efficiency of the energy transfer between these complexes. Apparently, a similar though less prominent effect also took place when *Rba. sphaeroides* chromatophores were treated with dipyridamole.

Since the membranes of isolated *Rba. sphaeroides* chromatophores retain closed vesicular structure and coupled energy-transduction systems, it is possible to study not only electron transport processes, but also conversion of the absorbed light energy into the energy of transmembrane charge separation. The shifts in carotenoid absorption bands in the spectral region of 400-500 nm arise in response to both local charge separations in the

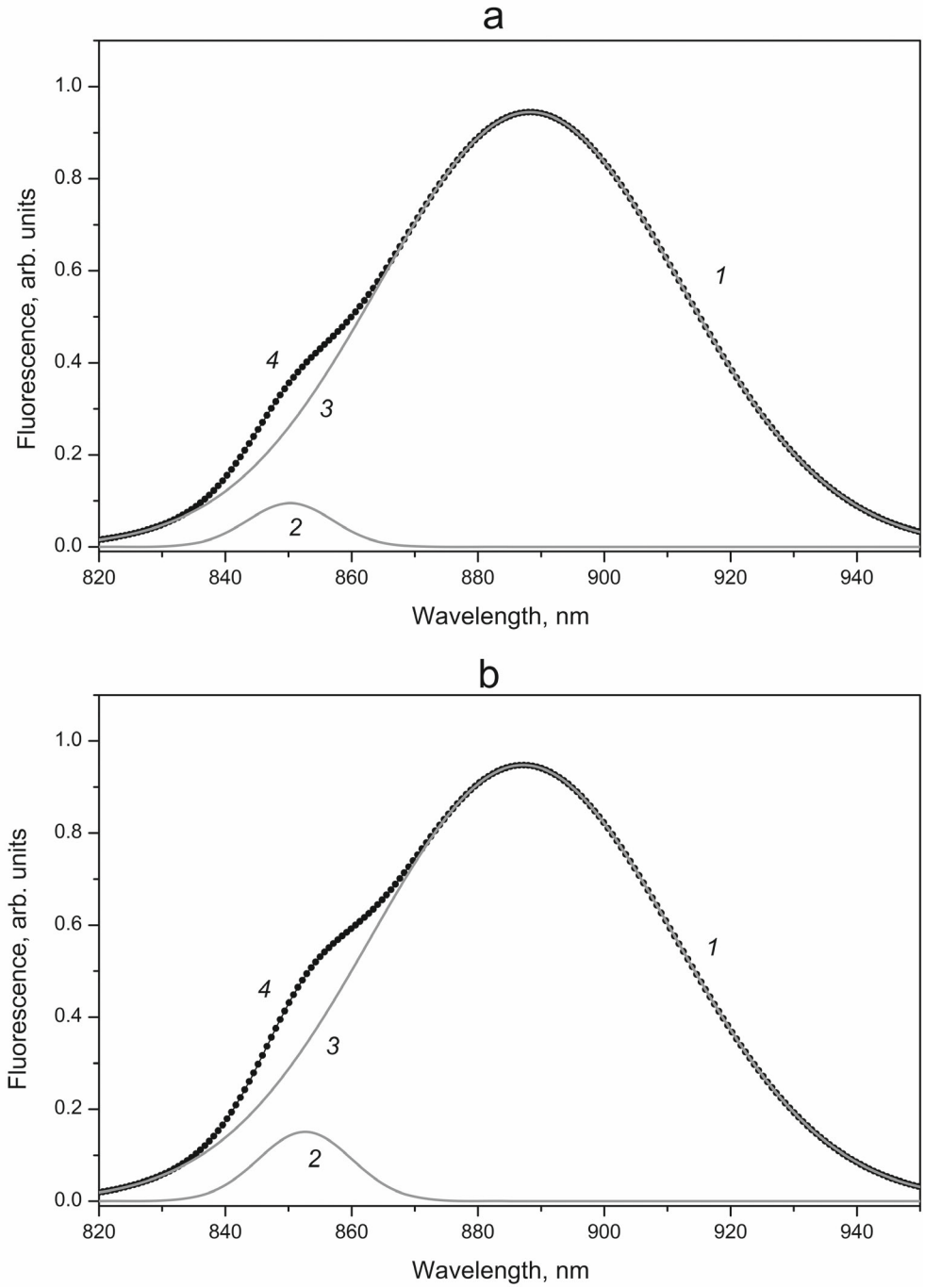

Fig. 1. Fluorescence spectra of a suspension of *Rba. sphaeroides* chromatophores (a) under control conditions and (b) in the presence of 1 mM DIP. Original spectra (dotted line *1*) were approximated by the sum of two Gaussian components (solid black curve *4*). The component with maximum near 855 nm (solid gray curve *2*) represents fluorescence of the LH2 complex, and the band with maximum at 890 nm (solid gray line *3*) displays fluorescence of the LH1 complex.

reaction centers and generation of transmembrane electric field that polarizes the protein matrix [23]. At the same time, the long-wavelength (so-called "red") shift of the absorption band of light-harvesting BChl molecules, observed in the IR spectral region at 840-900 nm, reflects mainly energization of the chromatophore membrane and is insensitive to the individual local electron transport steps at the chain segment $P \rightarrow Q_A \rightarrow Q_B$. These changes of absorbance were observed both in the whole cells of various species of purple bacteria and in the isolated chromatophores with closed vesicular structure, as in bacteria *R. rubrum*, *Rba. sphaeroides*, and *Ch. minutissimum* [24, 25]. This energy-dependent "red" shift in the BChl absorption was observed under conditions when the transmembrane electron transfer was accompanied by the antibiotic proton transport in the form of reduced secondary hydroquinone as a result of the Q-cycle operation involving the cytochrome bc_1 oxidoreductase

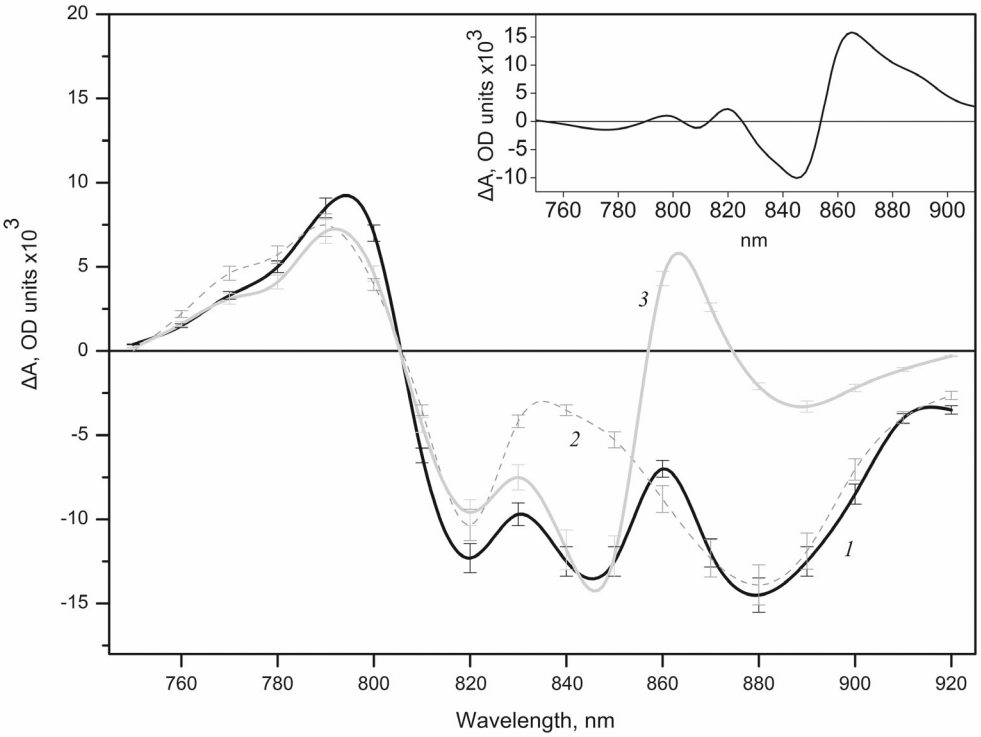

Fig. 2. Differential (light-minus-dark) spectra of *Rba. sphaeroides* chromatophores. Curves: *1*) under control conditions, *2*) in the presence of 10 mM of electron transfer inhibitor orthophenanthroline, and *3*) in the presence of 1 mM DIP. Differential "spectrum *3* minus spectrum *2*" after normalization of both spectra to absorption at 790 nm is shown in inset.

complex. When an exogenous electron donor (2,6-dichlorophenolindophenol, DCPIP, with excess ascorbate) was added to the medium, this red shift was enhanced under stationary light due to activation of the cyclic electron transport in those RCs where the electron donor cytochrome c_2 was absent.

At the same time, blocking of electron transport in the region between the primary and secondary quinone acceptors by means of specific inhibitor of o-phenanthroline led to the complete suppression of the red shift [26].

Figure 2 shows differential (light-minus-dark) absorption spectra of *Rba. sphaeroides* chromatophores under control conditions (*1*), after treatment with electron transfer inhibitor o-phenanthroline (*2*), and in the presence of DIP (*3*). The spectrum of the control sample in the near IR region comprises a positive peak at 790 nm and three negative maxima at 820, 840, and 880 nm. This type of spectrum indicated that the native structure of the chromatophore membranes was undisturbed and that generation of the electric potential difference at the membrane produced the "red" shift in the absorption band of the light-harvesting BChl. Since no exogenous electron donor was added, cyclic activity of the photosynthetic apparatus was apparently low, and no positive changes were observed in the region of 850-900 nm. After the blockage of electron transport by o-phenanthroline, only the absorption changes due to the pigment P photooxidation were retained. These changes were characterized by bleaching of the band at 870 nm and concomitant short-wavelength shift of the absorption band of monomeric BChl at 800 nm, with differential spectrum maximum at 790 nm and minimum at 820 nm (Fig. 2, curve *2*).

Addition of DIP enhanced the energy-dependent absorption changes. In the differential absorption spectrum, positive changes in the region of 850-900 nm with maximum around 860 nm were due to the superimposed redox changes of RC components (photooxidized P^+) and changes caused by the action of transmembrane electric field on light-harvesting BChl. This view is supported by the complex kinetics of the oppositely directed photoinduced absorption changes in the aforementioned spectral region after switching off the activating light. The kinetic curves indicate existence of the slowly relaxing "positive" and fast-relaxing "negative" absorption changes. The former changes are presumably associated with the "red" shift of the absorption of antenna pigments, and the latter are supposedly caused by the redox transformations of P. Light curves measured in the spectral region characteristic of only the second type of absorption changes (e.g., at 790 nm) and in the region where both types of changes are superimposed (around 860 nm) also confirm the above conclusion (Fig. 3). Data presented in Fig. 3 suggest that the positive photoinduced absorption changes associated with the long-wavelength shift of the BChl band due to the charge separation demonstrate saturation at lower light intensities than the negative absorption changes caused by the bleaching of photoactive P.

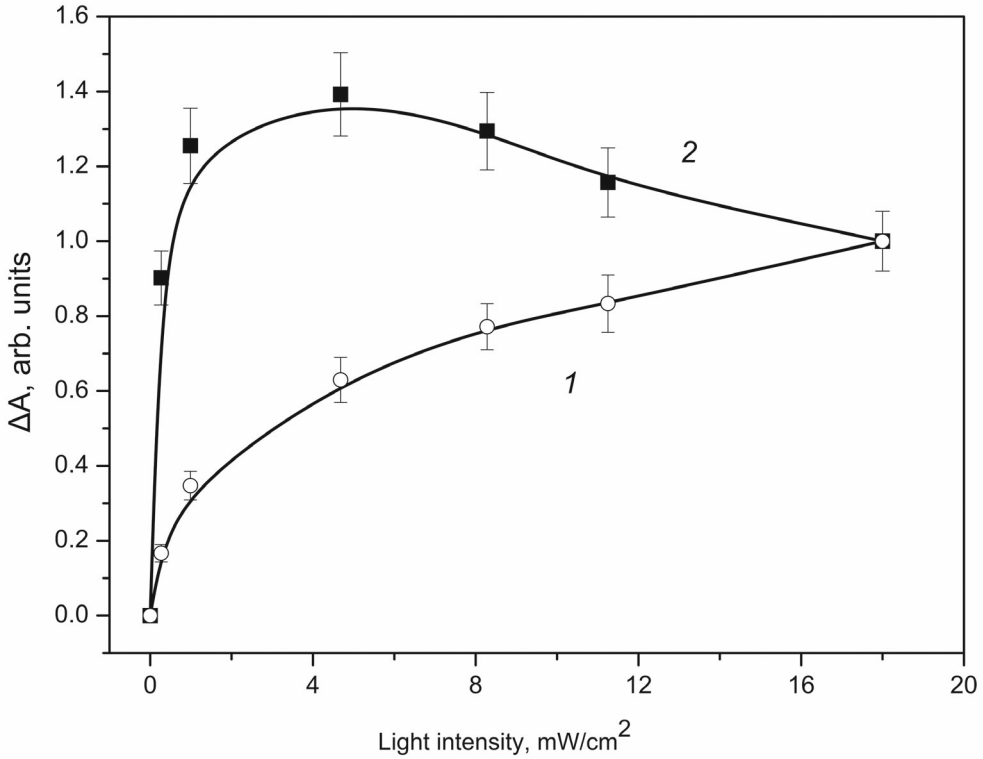

Fig. 3. Amplitudes of photoinduced absorbance changes in the chromatophores of *Rba. sphaeroides* in the presence of 1 mM DIP as a function of light intensity. Absorbance changes at 790 nm (curve *1*) reflect redox transformations of the photoactive P and absorbance changes at 860 nm (curve *2*) represent superposition of the redox conversions and energy-dependent red shift of the 850 nm band.

It should be pointed out that the field strength across the membrane can be as high as 10^8 V/m [27].

By subtracting spectrum *2* from spectrum *3* (see inset in Fig. 2) we obtain differential spectrum for the voltage-dependent absorption changes. Structure of the differential spectrum indicates that energization of the chromatophore membranes results in the long-wavelength shift of the absorption band of light-harvesting BChl molecules at 850 nm.

As noted above, *Rba. sphaeroides* contain two types of antenna complexes: LH2, i.e., molecules with absorption maxima at 800 and 850 nm (BChl 800-850), and LH1 with an absorption maximum at 870 nm (BChl 870). According to the X-ray diffraction data [28, 29], the BChl 850 molecules reside in a substantially hydrophobic environment; they are densely packed, and the planes of their porphyrin rings are oriented perpendicular to the plane of the chromatophore membrane. At the same time, the BChl 800 monomeric molecules are located between the outer helixes of the protein component; they are oriented parallel to the membrane plane, and interact with the polar medium. Perpendicular orientation of the BChl 850 molecules to the membrane plane and low dielectric constant of their membrane environment are apparently the main factors underlying the long-wavelength electrochromic shift of their absorption band (Stark effect) caused by the high-intensity electric field associated with generation of the transmembrane potential difference.

The effect of DIP on energization of the chromatophore membranes could be explained by assuming that this agent is capable of donating electrons to photooxidized P, similarly to the action of redox mediators DCPIP and TMPD in the presence of sodium ascorbate. Stimulating effect of the later chemicals on energization of the chromatophore membranes has long been known [25] and involves enhancement of the cyclic electron transport due to electron supply from the reduced form of TMPD to the photooxidized pigment P. The recorded dark reduction of P^+ is accelerated in this case.

Figure 4 shows kinetic curves of the photoinduced absorption changes in the chromatophores at 790 nm – spectral band indicative of the redox conversions – under control conditions and after addition of TMPD-H_2 or DIP.

As can be seen in Fig. 4, dark reduction of the pigment was substantially accelerated in both cases, which confirms the assumed electron-donor properties of DIP. However, these properties of DIP are much less pronounced compared to those of TMPD-H_2. The highest acceleration of the reduction kinetics in the presence of DIP was achieved at concentration of 1 mM. Further increase of DIP concentration did not accelerate dark reduction of P^+. It should be noted that the red shift of BChl 850 band manifested under continuous illumination as a positive absorption change at 860 nm also reached its highest value at DIP concentration of 1 mM.

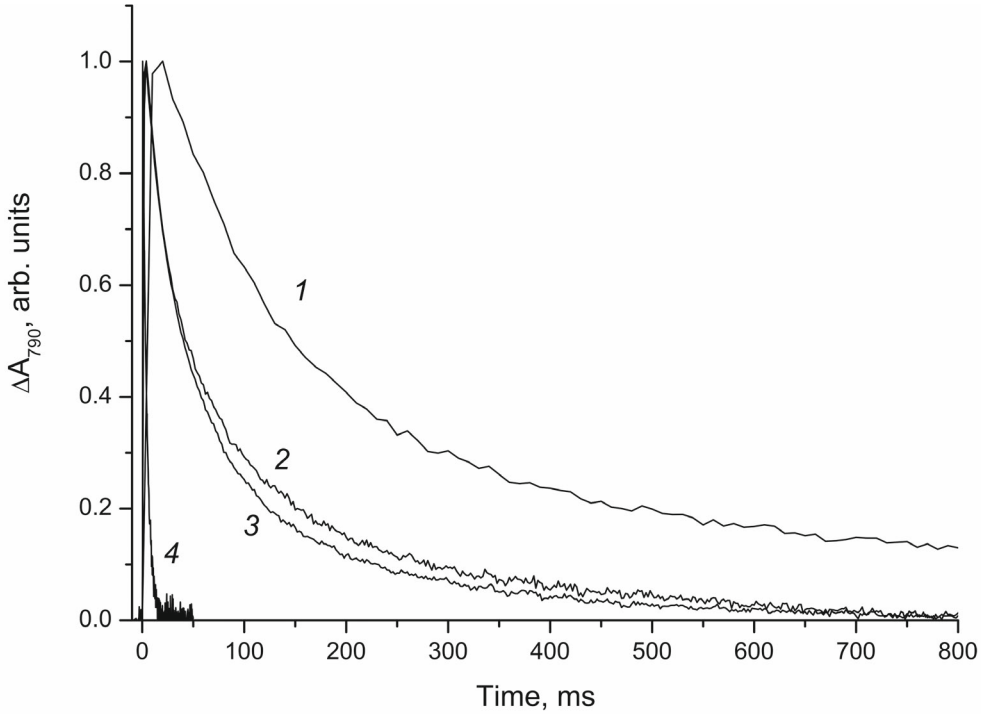

Fig. 4. Kinetics of P^+ dark reduction in the chromatophores of *Rba. sphaeroides* after activation with a single laser flash (532 nm, 7 ns) under control conditions (*1*), in the presence of 1 mM DIP (*2*), and in the presence of TMPD-H_2 at concentrations of 1 μM (*3*) and 1 mM (*4*).

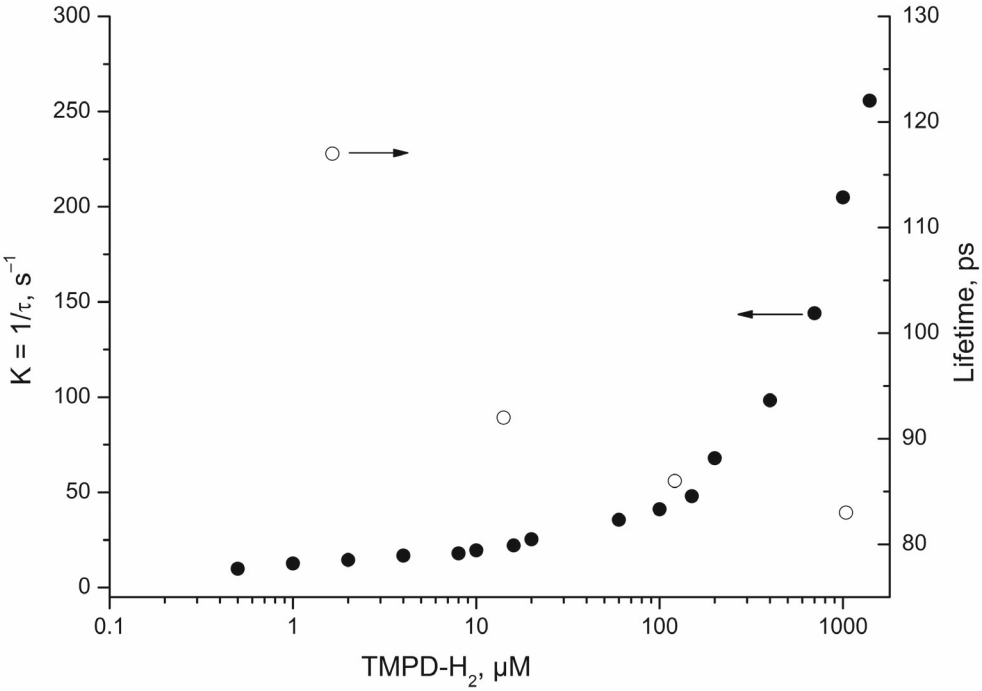

Fig. 5. Rate constants of P^+ dark reduction in the chromatophores of *Rba. sphaeroides* (black circles) after illuminating the sample with a laser flash (532 nm, 7 ns) in the presence of TMPD-H_2 at various concentrations. Calculations are based on the time during which the light-induced absorbance change decreased 2.7-fold. The graph also shows effect of TMPD-H_2 concentration on the decay time τ of the fast BChl fluorescence component (open circles) with amplitude of approximately 95%.

Obviously TMPD-H_2 is a much more efficient electron donor. At TMPD-H_2 concentration of ~1 μM the accelerated kinetics of P^+ reduction was already similar to that observed with 1 mM DIP; further addition of TMPD-H_2 to concentration of 1 mM substantially increased the rate constant of P^+ reduction (Fig. 5).

We also investigated changes of the fluorescence lifetime in the *Rba. sphaeroides* chromatophores upon

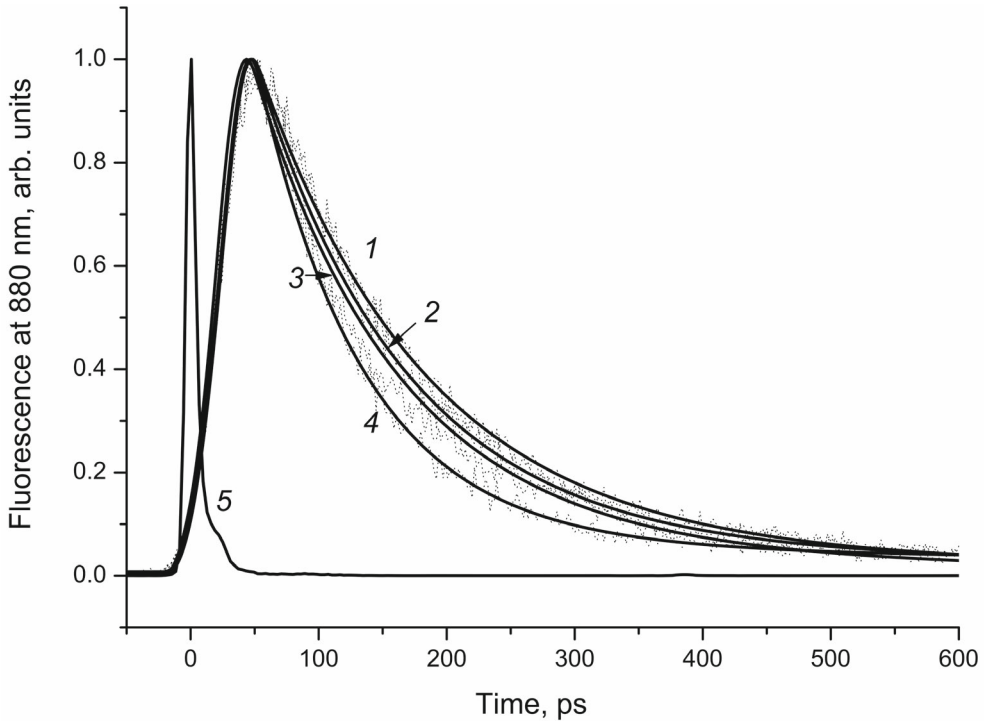

Fig. 6. Fluorescence decay kinetics in the chromatophores of *Rba. sphaeroides* under control conditions (*1*), in the presence of 1 mM DIP (*2*), and in the presence of TMPD-H_2 at concentrations of 1 μM (*3*) and 1 mM (*4*). Curve *5* is the instrumental function with width ~16 ps. Dots are experimental data; solid lines show the result of two-exponential approximation.

addition of DIP and TMPD-H_2 (Fig. 6, table, lifetimes and amplitudes of the fluorescence decay kinetics presented in the table were obtained with a two-exponential approximation).

As can be seen in Fig. 6, this kinetics is accelerated upon addition of both DIP and TMPD-H_2. This is explained as follows. Although the intensity of excitation light was very low, at the photoexcitation frequency of 80 MHz, when the light pulses follow every 12.5 ns, part of the photoactive pigment in the chromatophores exists permanently in the oxidized state (because, as noted above, initial cyclic activity of the photosynthetic apparatus evaluated from the red shift was low). Addition of the external electron donor TMPD-H_2 increases the level of reduction of the photoactive P in the course of these kinetic measurements.

It is known that lifetime of the fluorescence of LH1 antenna complexes depends significantly on the redox state of photoactive RC pigment. In the samples with reduced RCs, the fluorescence lifetime is ~80 ps. In the case of oxidized RCs, duration of the fast component of the fluorescence decay kinetics increases to ~200 ps. As can be seen from the kinetics in Fig. 6, the absorbed light energy was used more effectively in the photochemical reactions in RCs when DIP and TMPD-H_2 were added, and the recorded fluorescence lifetime was shorter.

Lifetimes (τ, ps) and amplitudes (a, %) of the fluorescence kinetic components* in the *Rba. sphaeroides* chromatophores under control conditions and in the presence of DIP and TMPD-H_2 at various concentrations

	Chromatophores of *Rba. sphaeroides*							
Lifetimes amplitudes	Control	+DIP, 0.1 mM	+DIP, 0.5 mM	+DIP, 1 mM	+TMPD, 1 μM	+TMPD, 10 μM	+TMPD, 100 μM	+ TMPD, 1 mM
τ_1	131 ± 6	125 ± 5	123 ± 5	112 ± 4	117 ± 6	92±6	86 ± 5	83 ± 4
τ_2	581 ± 17	602 ± 15	597 ± 15	616 ± 14	767 ± 15	873±16	878 ± 14	889 ± 14
a_1	96.0 ± 4.3	95.2 ± 4.7	94.2 ± 3.5	93.9 ± 4.4	95.2 ± 5.1	95.1±4.6	95.2 ± 3.9	94,9 ± 5,3
a_2	4.0 ± 0.8	4.8 ± 1.1	5.8 ± 0.9	6.1 ± 0.4	4.8 ± 0.9	4.9±0.7	4.8 ± 0.6	5,1 ± 1,0

* Data are presented as mean values and standard errors obtained for three measurements.

λ_{ex} = 400 nm, λ_{em} = 880 nm.

Based on the comparison of the effects of DIP and TMPD-H_2 on the fluorescence lifetime for isoeffective concentrations of these agents causing equal acceleration of P^+ reduction (1 mM and 1 μM, respectively), we can state that the effects are quite similar. However, lifetime τ of the fast component of the fluorescence kinetics continued to decrease at higher concentrations of TMPD-H_2, which corresponds to the results of the absorption measurements (Fig. 5). Extrapolation of the dependences shown in Fig. 5 yields a value of approximately 80 ps. Based on the literature data and the results of this work, we believe that the value of 80 ps is the time of excitation trapping in the LH1 complex by the reaction centers with the reduced photoactive pigment.

DISCUSSION

It should be noted that the accelerated delivery of excitation energy (by ~10%) to the photoactive RC pigment in the presence of DIP (Fig. 6) was accompanied by a certain decrease in the efficiency of energy transfer from LH2 to LH1–RC complexes. This is indicated by nearly 1.7-fold increase in the fluorescence intensity of LH2 complex with the maximum at 855 nm in the stationary fluorescence spectrum (Fig. 1) and simultaneous ~1.6-fold increase in the contribution of the slow (hundreds of picoseconds) component of the fluorescence decay kinetics recorded at 860 nm, which reflects intrinsic fluorescence of LH2 (data not shown). Comparing contributions of the slow component of fluorescence decay kinetics at 880 nm in the control samples and in the preparations supplemented with 1 mM DIP (table) leads us to the same conclusion. Importantly, addition of TMPD-H_2 causes reduction of only the lifetime of the fast (~100 ps) component, while the ratio of amplitudes of the two phases remained almost unaffected. It is possible that DIP disrupts spatial packing of lipids, leading to the changes in mutual arrangement of LH2 and LH1–RC complexes. We have previously observed a similar phenomenon when the photosynthetic membranes of *Rba. sphaeroides* were exposed to cationic antiseptics [22]. This analogy may be due to the similar modifying effects of antiseptics and DIP on biomembranes. The effects of cationic antiseptics involve charge interactions with the membrane surface, because positive charges on the nitrogen atoms are spatially separated in the molecular structure of these agents. Under experimental conditions used, dipyridamole molecules also generated a cation radical with the positive charges localized on nitrogen atoms.

While discussing the electron-donor capabilities of DIP, it should be noted that the mechanism of DIP oxidation is still a controversial issue. According to the results of voltammetric studies [30], oxidation of DIP in aqueous solutions comprises either two consecutive events controlled by one-electron diffusion or one-step oxidation involving two electrons. Stoichiometry of the anodic oxidation of DIP in aqueous solutions corresponds to the detachment of two electrons from each DIP molecule, which is accompanied by the release of one proton per oxidized molecule [31]. It is assumed in [32] that electrooxidation of DIP results in reorganization of the piperidine rings, which leads to the appearance of a positive charge on their nitrogen atoms. Donation of electrons by DIP molecule into the electron transport chain of RC cofactors is accompanied by formation of the reduced hydroquinone (quinol) Q_B-H_2. The latter enters the membrane, being rapidly replaced by ubiquinone-10 from the membrane pool, the size of which equals to 20-30 ubiquinone molecules per the reaction center [33, 34]. Oxidation of ubiquinol by the cytochrome bc_1 membrane complex in the presence of molecular oxygen can produce superoxide anion [35]. Consumption of molecular oxygen during this reaction by the chromatophore membranes of purple bacteria under conditions of cyclic electron transport was demonstrated long ago [36]. The superoxide produced in the membrane can react with DIP. The latter reaction was demonstrated in our work with preparations of the isolated RCs capable of generating superoxide radicals under continuous illumination [37]. Quenching of free radicals by DIP molecules could be caused, among other things, by the proton transfer coupled with the detachment of an electron from various nitrogen atoms [13].

According to the modern concepts [38], complete reaction cycle of the cytochrome bc_1 complex comprises oxidation of two quinol molecules with production of two quinone molecules. These reactions proceed at the Q_o site of the cytochrome bc_1 complex on the membrane side that is opposite to the location of the quinone acceptor site of the RC. Next, the two electrons out of four from the Q_o site reduce the mobile electron carrier, cytochrome c_2 involved in the reduction of photooxidized P^+. The other two electrons reduce one quinone molecule from the membrane pool to quinol in the Q_i site of the complex on the other side of the membrane. The latter reaction is accompanied by the additional uptake of two protons from the medium. In the presence of molecular oxygen, O_2 easily diffuses into the cytochrome bc_1 complex, where it can be reduced in a side reaction to superoxide at the Q_o site [38]. Also, molecular oxygen can itself accept a hydrogen atom from a quinol molecule [35], thus producing protonated superoxide (O_2·H). The latter diffuses into the aqueous phase and generates superoxide via deprotonation.

In our experiments, transfer of electrons to oxygen and protonation of the produced superoxide by DIP molecules are probably one of the sources for energization of photosynthetic membrane observed upon activation of chromatophores by continuous light. Energization seems to be the result of uptake and transmembrane movement

of protons by the functional cytochrome bc_1 complex. It is also likely that the electron-donating ability of DIP promotes the light-induced cyclic transport involving water-soluble mobile molecules of cytochrome c_2. The latter molecules are partially lost during the isolation of chromatophores [39]. This loss may account for the initially low cyclic activity in the preparations of chromatophores (Fig. 2, curve *1*).

CONCLUSIONS

In summary it can be stated that the results of this study confirm that the mechanisms discussed in the literature for the effects of DIP on the interactions of membrane proteins and the electron-donor properties of DIP could indeed affect activity of the functional membrane proteins. This provides additional motivation for considering the analyzed possibilities when studying the mechanisms of therapeutic effects of DIP, including its effect on the activity of the transmembrane protein P-gp that facilitates multiple antitumor drug resistance.

Contributions. P. P. Knox, E. P. Lukashev, and V. Z. Paschenko formulated the problem, discussed the results, and wrote the manuscript; E. P. Lukashev, B. N. Korvatovskii, S. N. Goryachev, and E. S. Allakhverdiev conducted experiments and processed the results; and N. Kh. Seifullina prepared biological samples for the research.

Funding. This work was financially supported by the State Budget Project of the Russian Federation (no. 121032500058-7).

Ethics declarations. The authors declare no conflict of interests in financial or any other sphere. This article does not contain any studies involving humans or animals performed by any of the authors.

REFERENCES

1. Jensen, B. O., Kleppe, R., Kopperud, R., and Nygaard, G. (2010) Dipyridamole synergizes with nitric oxide to prolong inhibition of thrombin-induced platelet shape change, *Platelets*, **22**, 8-19, doi: 10.3109/09537104.2010.517581.
2. Shalinsky, D. R., Andreef, M., and Howell, S. B. (1990) Modulation of drug sensitivity by dipyridamole in multidrug resistant tumor cells *in vitro*, *Cancer Res.*, **50**, 7537-7543.
3. Iuliano, L., Colavita, A. R., Leo, R., Praticò, D., and Violi, F. (1997) Oxygen free radicals and platelet activation, *Free Radic. Biol. Med.*, **22**, 999-1006, doi: 10.1016/s0891-5849(96)00488-1.
4. Wessler, J. D., Grip, L. T., Mendell, J., and Giugliano, R. P. (2013) The P-glycoprotein transport system and cardiovascular drugs, *J. Americ. Coll. Cardiol.*, **61**, 2495-2502, doi: 10.1016/j.jacc.2013.02.058.
5. Aliter, K. F., and Al-Horani, R. A. (2021) Potential therapeutic benefits of dipyridamole in COVID-19 patients, *Curr. Pharm. Des.*, **27**, 866-875, doi: 10.2174/1381612826666201001125604.
6. Liu, X., Li, Z., Liu, S., Sun, J., Chen, Z., et al. (2020) Potential therapeutic effects of dipyridamole in the severely ill patients with COVID-19, *Acta Pharm. Sin. B*, **10**, 1205-1215, doi: 10.1016/j.apsb.2020.04.008.
7. Knox, P. P., Churbanova, I. Yu., Lukashev, E. P., Zakharova, N. I., Rubin, A. B., et al. (2000) Dipyridamole and its derivatives modify the kinetics of the electron transport in reaction centers from *Rhodobactersphaeroides*, *J. Photochem. Photobiol.*, **56**, 68-77, doi: 10.1016/s1011-1344(00)00062-2.
8. Knox, P. P., Lukashev, E. P., Mamedov, M. D., Semenov, A. Yu., Seifullina, N. Kh., et al. (2000) Slowing of proton transport processes in the structure of bacterial reaction centers and bacteriorhodopsin in the presence of dipyridamole, *Biochemistry (Moscow)*, **65**, 213-217.
9. Knox, P. P., Lukashev, E. P., Mamedov, M. D., Semenov, A. Yu., and Borissevitch, G. P. (2001) Proton transfer in bacterial reaction centers and bacteriorhodopsin in the presence of dipyridamole, *Prog. React. Kinet. Mech.*, **26**, 287-298, doi: 10.3184/007967401103165217.
10. Iuliano, L., Pratico, D., Ghiselli, A., Bonavita, M. S., and Violi, F. (1992) Reaction of dipyridamole with the hydroxyl radical, *Lipids*, **27**, 349-353, doi: 10.1007/BF02536149.
11. Nepomuceno, M. F., Alonso, A., Pereira-Da-Silva, L., and Tabak, M., (1997) Inhibitory effect of dipyridamole and its derivatives on lipid peroxidation in mitochondria, *Free Radic. Biol. Med.*, **23**, 1046-1054, doi: 10.1016/s0891-5849(97)00135-4.
12. Almeida, L. E., Castilho, M., Mazo, L. H., and Tabak, M. (1998) Voltammetric and spectroscopic studies of the oxidation of the anti-oxidant drug dipyridamole in acetonitrile and ethanol, *Anal. Chim. Acta*, **375**, 223-231, doi: 10.1016/S0003-2670(98)00501-7.
13. Barzegar, A. (2012) Proton-coupled electron-transfer mechanism for the radical scavenging activity of cardiovascular drug dipyridamole, *PLoS One*, **7**, e39660, doi: 10.1371/journal.pone.0039660.
14. Galati, G., and O'Brien, P. J. (2004) Potential toxicity of flavonoids and other dietary phenolics: significance for their chemopreventive and anticancer properties, *Free Radic. Biol. Med.*, **37**, 287-303, doi: 10.1016/j.freeradbiomed.2004.04.034.
15. Knox, P. P., Timofeev, K. N., Gorokhov, V. V., Seifullina, N. Kh., and Rubin, A. B. (2017) Generation of radical form of dipyridamole at illumination of photosynthetic reaction centers of *Rb. sphaeroides*, *Dokl. Biochem. Biophys.*, **473**, 118-121, doi: 10.1134/S1607672917020089.
16. Knox, P. P., Lukashev, E. P., Seyfullina, N. Kh., Gorokhov, V. V., and Rubin, A. B. (2017) The influence of dipyridamole and its derivatives on the membrane energization state of *Rhodobacter sphaeroides* bacterial chromatophores, *Biophysics*, **62**, 734-741.

17. Cartron, M. L., Olsena, J. D., Sener, M., Jackson, P. J., Brindley, A. A., et al. (2014) Integration of energy and electron transfer processes in the photosynthetic membrane of *Rhodobactersphaeroides*, *Biochim. Biophys. Acta*, **1837**, 1769-1780, doi: 10.1016/j.bbabio.2014.02.003.
18. Sundström, V., Pullerits, T., and van Grondelle, R. (1999) Photosynthetic light harvesting: reconciling dynamics and structure of purple bacterial LH2 reveals function of photosynthetic unit, *J. Phys. Chem. B*, **103**, 2327-2346, doi: 10.1021/jp983722+.
19. Freiberg, A., Allen, J. P., Williams, J. A. C., and Woodbury, N. W. (1996) Energy trapping and detrapping by wild type and mutant reaction centers of purple non-sulfur bacteria, *Photosyn. Res.*, **48**, 309-319, doi: 10.1007/BF00041022.
20. Driscoll, B., Lunceford, C., Lin, S., Woronowicz, K., Niederman, R. A., and Woodbury, N. W. (2014) Energy transfer properties of *Rhodobactersphaeroides* chromatophores during adaptation to low light intensity, *Phys. Chem. Chem. Phys.*, **16**, 17133-17141, doi: 10.1039/C4CP01981D.
21. Caycedo-Soler, F., Rodrigez, F. J., Quiroga, L., Zhao, G., and Johnson, N. F. (2011) Energy conversion in purple bacteria photosynthesis, in *Photosynthesis* (Najafpour, M., ed.) INTECH, London, pp. 1-27, doi: 10.5772/26241.
22. Strakhovskaya, M. G., Lukashev, E. P., Korvatovskiy, B. N., Kholina, E. G., Seifullina, N. Kh., et al. (2021) The effect of some antiseptic drugs on the energy transfer in chromatophore photosynthetic membranes of purple non-sulfur bacteria *Rhodobactersphaeroides*, *Photosyn. Res.*, **147**, 197-209, doi: 10.1007/s11120-020-00807-x.
23. Andersson, P. O., Gillbro, T., Ferguson, L., and Cogdell, R. J. (1990) Spectral shift of purple bacterial carotenoids related to solvent and protein polarizability, in Current Research in Photosynthesis (Baltscheffsky, M., ed.) Vol. II, Kluwer Academic Publishers, Dordrecht, pp. 117-120.
24. Vredenberg, V. J., and Amesz, J. (1966) Absorption bands of bacteriochlorophyll types in purple bacteria and their response to illumination, *Biochim. Biophys. Acta*, **126**, 244-261, doi: 10.1016/0926-6585(66)90060-4.
25. Barsky, E. L., and Samuilov, V. D. (1979) Blue and red shifts of bacteriochlorophyll absorption band around 880 nm in *Rhodospirillum rubrum*, *Biochim. Biophys. Acta*, **548**, 448-457, doi: 10.1016/0005-2728(79)90057-4.
26. Kononenko, A. A., Venediktov, P. S., Chemeris, Yu. K., Adamova, N. P., and Rubin, A. B. (1974) Relation between electron transport-linked processes and delayed luminescence in photosynthesizing bacteria, *Photosynthetica*, **8**, 176-183.
27. Junge, W. (1977) Membrane potentials in photosynthesis, *Ann. Rev. Plant Physiol.*, **28**, 503-536, doi: 10.1146/annurev.pp.28.060177.002443.
28. McDermot, G., Prince, S. M., Freer, A. A., Hawthornthwaite-Lawless, A. M., Papiz, M. Z., et al. (1995) Crystal-structure of an integral membrane light-harvesting complex from photosynthetic bacteria, *Nature*, **374**, 517-521, doi: 10.1038/374517a0.
29. Poszak, A. W., Howard, T. D., Soutal, J., Gurdiner, A. T., Low, C. J., et al. (2003) Crystal structure of the RC-LH1 core complex from *Rhodopseudomonas palustris*, *Science*, **302**, 1969-1972, doi: 10.1126/science.1088892.
30. Tabak, M., Castilho, M., Almeida, L. E., and Mazo, L. H. (1998) Voltammetric studies of dipyridamole oxidation in aqueous micellar solutions, *Free Radic. Biol. Med.*, **25**, S40, doi: 10.1016/S0891-5849(98)90119-8.
31. Castilho, M., Almeida, L. E., Tabak, M., and Mazo, L. H. (2000) Voltammetric oxidation of dipyridamole in aqueous acid solutions, *J. Braz. Chem. Soc.*, **11**, 148-153, doi: 10.1590/S0103-50532000000200008.
32. David, I. G., Iordache, L., Popa, D. E., Buleandra, M., David, V., et al. (2019) Novel voltammetric investigation of dipyridamole at a disposable pencil graphite electrode, *Turk. J. Chem.*, **43**, 1109-1122, doi: 10.3906/kim-1903-64.
33. Crofts, A. R., and Wraight, C. A. (1983) The electrochemical domain of photosynthesis, *Biochim. Biophys. Acta*, **726**, 149-185, doi: 10.1016/0304-4173(83)90004-6.
34. Mezzettia, A., Leibla, W., Breton, J., and Nabedryk, E. (2003) Photoreduction of the quinone pool in the bacterial photosynthetic membrane: identifcation of infrared marker bands for quinol formation, *FEBS Lett.*, **537**, 161-165, doi: 10.1016/s0014-5793(03)00118-2.
35. Yin, Y., Yang, S., Yu, L., and Yu, C.-A. (2010) Reaction mechanism of superoxide generation during ubiquinol oxidation by the cytochrome bc_1 complex, *J. Biol. Chem.*, **285**, 17038-17045, doi: 10.1074/jbc.M110.104364.
36. Remennikov, V. G., and Samuilov, V. D. (1980) Interaction of photosynthetic electron transport chain components *Rhodospirillum rubrum* with oxygen, *Dokl. Akad. Nauk SSSR*, **252**, 491-494.
37. Knox, P. P., Lukashev, E. P., Timofeev, K. N., and Seifullina, N. Kh. (2002) Effects of oxygen on the dark recombination between photoreduced secondary quinone and oxidized bacteriochlorophyll in *Rhodobacter sphaeroides*reaction centers, *Biochemistry (Moscow)*, **67**, 901-907, doi: 10.1023/a:1019966620850.
38. Husen, P., and Solov'yov, I. A. (2016) Spontaneous binding of molecular oxygen at the Q_o-site of the bc1 complex could stimulate superoxide formation, *J. Am. Chem. Soc.*, **138**, 12150-12158, doi: 10.1021/jacs.6b04849.
39. Michels, P. A. M., and Konings, W. N. (1978) Structural and functional properties of chromatophores and membrane vesicles from *Rhodepseudomonas sphaeroides*, *Biochim. Biophys. Acta*, **507**, 353-368, doi: 10.1016/0005-2736(78)90346-2.